

HOSTED BY



Contents lists available at ScienceDirect

Saudi Pharmaceutical Journal

journal homepage: [www.sciencedirect.com](http://www.sciencedirect.com)

Original article

# QbD driven targeted pulmonary delivery of dexamethasone-loaded chitosan microspheres: Biodistribution and pharmacokinetic study

B.R. Asha<sup>a,1</sup>, Prakash Goudanavar<sup>a,1</sup>, G.S.N. Koteswara Rao<sup>b</sup>, Kumaraswamy Gandla<sup>c</sup>,  
N. Raghavendra Naveen<sup>a,\*</sup>, Shahnaz Majeed<sup>d</sup>, Ravindran Muthukumarasamy<sup>d,\*</sup>

<sup>a</sup> Department of Pharmaceutics, Sri Adichunchanagiri College of Pharmacy, Adichunchanagiri University, B.G. Nagar, Karnataka 571448, India

<sup>b</sup> Department of Pharmaceutics, Shobhaben Pratapbhai Patel School of Pharmacy & Technology Management, SVKM's NMIMS, Vile Parle (W), Mumbai 400056, Maharashtra, India

<sup>c</sup> Department of Pharmaceutical Analysis, Chaitanya (Deemed to be University), Hanamkonda 506001, Telangana, India

<sup>d</sup> Faculty of Pharmacy and Health Sciences, Universiti Kuala Lumpur Royal college of Medicine Perak, No 3, Jalan Green town, Ipoh 30450, Perak, Malaysia

## ARTICLE INFO

### Article history:

Received 29 May 2023

Accepted 20 July 2023

Available online 26 July 2023

### Keywords:

Pulmonary delivery

Quality by design

Microparticles

Chitosan

Dexamethasone

## ABSTRACT

Inhaling drugs, on the other hand, is limited mainly by the natural mechanisms of the respiratory system, which push drug particles out of the lungs or make them inefficient once they are there. Because of this, many ways have been found to work around the problems with drug transport through the lungs. Researchers have made polymeric microparticles (MP) and nanoparticles as a possible way to get drugs into the lungs. They showed that the drug could be trapped in large amounts and retained in the lungs for a long time, with as little contact as possible with the bloodstream. MP were formulated in this study to get dexamethasone (DMC) into the pulmonary area. The Box-Behnken design optimized microspheres preparation to meet the pulmonary delivery prerequisites. Optimized formulation was figured out based on the desirability approach. The mass median aerodynamic diameter (MMAD) of the optimized formula (O-DMC-MP) was  $8.46 \pm 1.45 \mu\text{m}$ , and the fine particle fraction (FPF) was  $77.69 \pm 1.26\%$ . This showed that it made suitable drug delivery system, which could make it possible for MP to settle deeply in the lung space after being breathed in. With the first burst of drug release, it was seen that drug release could last up to 16 h. Also, there was no clear sign that the optimized formulation was toxic to the alveoli basal epithelial cells in the lungs, as supported by cytotoxic studies in HUVEC, A549, and H1299 cell lines. Most importantly, loading DMC inside MP cuts the amount of drug into the bloodstream compared to plain DMC, as evident from biodistribution studies. Stability tests have shown that the product can stay the same over time at both the storage conditions. Using chitosan DMC-MP can be a better therapeutic formulation to treat acute respiratory distress syndrome (ARDS).

© 2023 The Author(s). Published by Elsevier B.V. on behalf of King Saud University. This is an open access article under the CC BY-NC-ND license (<http://creativecommons.org/licenses/by-nc-nd/4.0/>).

## 1. Introduction

Particle drug delivery methods are becoming more important in clinical medicine and pharmacology research. Microspheres (MP) are small, round particles with sizes from 1 to 1000  $\mu\text{m}$  (Rowley

et al., 1999). MP can be made from various polymeric materials, both natural and semi-synthetic, or even from artificial materials. As drug delivery systems, MP have several significant benefits, such as protecting the encapsulated active agent from being broken down by enzymes; being able to precisely control the rate at which the encapsulated drug is released over timescales ranging from hours to months; and being easy for administration (compared to other parenteral controlled release dosage forms, and large implants etc.). Emulsion crosslinking is one of the most common methods used in the pharmaceutical formulation for microencapsulation, which is sensitive to heat and improves the way granules flow (Anandharamakrishnan et al., 2007). Emulsion crosslinking is an easy-to-find, fast, and ongoing way to turn a solution or dispersion into solid particles like granules or MP. Various process parameters always determine the nature of the prepared formulation (Ezhilarasi et al., 2014).

\* Corresponding authors.

E-mail addresses: [raghavendra.naveen@gmail.com](mailto:raghavendra.naveen@gmail.com) (N. Raghavendra Naveen), [shahnaz@unikl.edu.my](mailto:shahnaz@unikl.edu.my) (S. Majeed), [ravindran@unikl.edu.my](mailto:ravindran@unikl.edu.my) (R. Muthukumarasamy).

<sup>1</sup> Authors contributed equally.

Peer review under responsibility of King Saud University.



Production and hosting by Elsevier

<https://doi.org/10.1016/j.jsps.2023.101711>

1319-0164/© 2023 The Author(s). Published by Elsevier B.V. on behalf of King Saud University.

This is an open access article under the CC BY-NC-ND license (<http://creativecommons.org/licenses/by-nc-nd/4.0/>).

“Quality by Design” (QbD) is the pharmaceutical industry’s magic bullet for obtaining the most sought-after product with the most desirable qualities while simultaneously making it easier to overcome regulatory barriers. The goals QbD approach to product development are to guarantee steady improvements in production and attest to the realization of an intended level of quality in the final product (Rathore and Winkle, 2009) completion of an intended level of quality in the final product (Rathore and Winkle, 2009). A subset of QbD called the Design of Experiments (DoE) offers a mathematical justification for the undefined parameters that emerge during the formulation development process. By delving deeper into DoE, a manufacturer can identify the critical attributes of the materials and the process parameters that will allow them to meet the specified essential quality characteristics (Yu et al., 2014). The QbD technique helps optimize the formulation characteristics of several drug delivery systems, including MP, nanosystems (Charoo et al., 2012), transdermal, etc., according to several recent findings (Aldawsari et al., 2022; Baldinger et al., 2012; Hosny et al., 2022).

Pulmonary illnesses are the third most common reason people die around the world. They include cough, cold, asthma, bronchitis, and more severe diseases. Some of the most common things in the pulmonary area are lung infections, high blood pressure in the airways, and the production of cytokines. Pulmonary drug transport is an excellent way to get drugs to work locally and throughout the body (Dolma Gurung and Kakar, 2020). But, to make a perfect pulmonary drug transport system, there is a need to know the factors that affect it, such as the cause, the pathophysiology, and the different barriers (mechanical, chemical, immunological, and behavioral). Formulation techniques and how particles settle in the lungs are essential for sound delivery. Several pieces of literature have shown the efficiency of pulmonary drug delivery systems by formulating various dosage forms (Cipolla et al., 2014; Karimi et al., 2018; Torge et al., 2019; Wang et al., 2022).

Because of its biodegradability, biocompatibility, and low toxicity, the natural carbohydrate polymer chitosan has long been studied for drug delivery and medical uses. Hydrolysis, oxidation, and enzymatic processes are the usual processes in the degradation of polymers. Degradation of chitosan, which is often hydrolyzed by enzymes lysozyme (which is accessible in the human body, particularly in the lungs) and chitinase, has been validated by a small number of earlier publications. Enzymes that break down glucosamine-glucosamine, glucosamine-N-acetyl-glucosamine, and N-acetyl-glucosamine-N-acetyl-glucosamine bonds can also degrade chitosan. Chitosan can be seen to degrade into its component monomers (D-glucosamine and N-acetyl-glucosamine) (Islam et al., 2019; Kean and Thanou, 2010; Rasul et al., 2020).

Acute respiratory distress syndrome (ARDS) is a group of symptoms caused by lung emphysema (Powers, 2022). Most often, ARDS is caused by bacterial pneumonia or pneumonia caused by a virus. ARDS can also be caused by sepsis in places other than the lungs, severe trauma, or breathing in stomach contents. (Ferguson et al., 2012). There are between 5 and 35 cases of ARDS for every 100,000 people in the United States each year, depending on the standards used and how the studies were done (Villar et al., 2016). Even though this syndrome has been studied in the lab and in people for 50 years, there is still no helpful drug therapy (Rubinfeld et al., 2005). Supportive care, like lung-protective ventilation and a cautious approach to controlling fluids, is still the primary treatment (Máca et al., 2017). Because of this, it is essential to study better ways of formulating various novel drug delivery systems. Dexamethasone (DMC), a corticosteroid, slows down the inflammatory process caused by glucocorticoid receptors (Abraham et al., 2006). This helps the body eliminate the disease

by reducing inflammation and speeding up tissue balance (Waljee et al., 2017). But taking low doses of dexamethasone for a long time can cause significant side effects (Bleecker et al., 2020). So, to treat ARDS, there needs to be a way to target the pulmonary region through specific drug delivery systems such as MP. With all the specified insights, this work aimed to optimize DMC polymeric MP that can be injected into the lungs and could improve the effectiveness of therapy in treating ARDS.

## 2. Materials and methods

### 2.1. Materials

Aurobindo Pharma of Hyderabad, India, generously donated to DMC. Sigma Aldrich (India) was contacted for chitosan, liquid paraffin, and glutaraldehyde, all of which were used in their pure forms. All of the other solvents and compounds are of analytical quality.

### 2.2. Preparation and optimization of DMC-loaded MP (DMC-MP)

The DMC-loaded chitosan MP was made with a simple method called water-in-oil (W/O) emulsion crosslinking (Wang et al., 2014), which is easy to scale up. In short, about 250 mg of chitosan and 20 mg of DMC were put into 10 mL of a mixture of acetic acid and ethanol that was 3:2 (v/v) in volume (Acetic acid with a concentration of up to 70% by weight is used to prepare chitosan solution). After fully dissolved, the solution was added slowly to a certain amount of liquid paraffin with span-80 and quickly mixed to make a water-in-oil emulsion. Then, a solution of glutaraldehyde (10%) was slowly added to the emulsion system and cross-linked for 3 h until the microspheres got hardened. The microspheres formed were, then filtered, and dried. The microspheres were passed through a 20 m sieve and washed three times with cold water. To prevent the sticking of MP to each other, water with 20% mannitol was added. Then they were separated after freeze-drying. One of the carriers employed in MP preparation, mannitol, increases MP deposition in the lungs’ lower airways, a finding validated by the formulation’s efficacy as an aerosol.

A statistical method was used to find the best way to make DMC-MP. The concentrations of liquid paraffin (ml) (X1), glutaraldehyde (%v/v) (X2), and Span-80 (g) (X3) were some of the independent factors that were chosen at. The codes –1, 0, and +1 show the low, medium, and high levels for each of the three factorial levels for each of these factors (Islam et al., 2022; Naveen et al., 2013; Rizg et al., 2022; Sreeharsha et al., 2022). Particle size (PS-Y1) and the Entrapment efficacy (EE-Y2) were chosen as dependent factors (Table 1).

### 2.3. Characterization of DMC-MP

#### 2.3.1. PS determination

The PS and polydispersity index were determined using the dynamic light scattering technique and a Malvern nano ZS 90 zeta sizer (Malvern Instrument, Worcestershire, UK). Using Milli-Q water, 100 mL samples were converted into 1 µL samples at 25 °C, and the particle size was determined (Nair et al., 2021; Sreeharsha et al., 2021).

#### 2.3.2. Determination of drug loading and EE

50 mg of DMC-MP was mixed with 40 mL of methanol, and then the mixture was shaken for 30 min with a Vortex sonicator. After that, the liquid formulation was put through a filter. High-Performance Liquid Chromatography (HPLC, Shimadzu, Kyoto, Japan) was used to measure the amount of DMC calculated

**Table 1**  
Box-Behnken optimization design for DMC-MP.

Independent variables	The level used, actual and coded		
	Low (-1)	Medium (-1)	High (-1)
X1 = Liquid paraffin (ml)	10	20	30
X2 = Glutaraldehyde (%v/v)*	10	25	40
X3 = Span-80 (g)	0.25	0.5	0.75
Dependent variables	<b>Goal</b>		
PS (Y1)EE (Y2)	MinimizeMaximize		

\* - Microspheres had a glutaraldehyde content of 0.1 ppm. The Occupational Safety and Health Administration has set the safe level of glutaraldehyde exposure at 0.8 mg/m<sup>3</sup> (0.2 ppm).

(Brugnera et al., 2022; Heda et al., 2011) (Hagbani et al., 2022). A 250 × 4.6 mm and 5 μm wide Qualisil C18 column was used for chromatographic separation. The mobile phase was made of a solution of weak orthophosphoric acid and acetonitrile with a pH of 3.0 that was mixed at a ratio of 60:40 (v/v). Before determining how much, the mobile phase was used to heat the column for 1 h to 40 °C. The UV monitor was set to 242 nm, and the flow rate was 1 mL/min. The following equations were used to figure out the accurate drug loading and drug encapsulation efficiency:

$$\text{Drug loading (\%)} = \frac{\text{Weight of drug in microspheres}}{\text{Weight of microspheres}} \times 100$$

$$\text{EE (\%)} = \frac{\text{Drug content in microspheres}}{\text{Initial drug content}} \times 100$$

#### 2.4. Characterization of optimized formulation of DMC-MP (O-DMC-MP)

##### 2.4.1. Microsphere surface morphology

With tungsten thermionic emission, scanning electron microscopy (SEM) (Tescan, Vega 35BH, Brno, Czech Republic) was used to look at the surface shape of the best microsphere makeup (Harsha et al., 2015b; Shah et al., 2019).

##### 2.4.2. In vitro deposition by Andersen cascade impactor

The aerodynamic characteristics of dry powder inhalers that have been ingested are frequently studied in vitro using the Andersen cascade impactor. Seven capsules containing 50 mg of drug-loaded microspheres each were used to measure the aerodynamic diameter of the O-DMC-MP. A linked inhaler to the cascade impactor was then filled with the capsules. Pellets containing medications were delivered to the impactor at a rate of 28.3 L/min for 10 s. The drug particles lodged on each stage of the cascade impactor were examined using HPLC equipment. The fine particle dosage, fine particle fraction (FPF), and released dose (FPD) were also used to explain the O-DMC-MP deposition curve (Hagbani et al., 2022). The FPF and FPD figures indicate the percentage and the dose of medication particles that made it to the pulmonary alveoli, respectively. Better aerosolization performance can be expected from an MDI with greater FPF and FPD values. Half of the particles' masses are bigger than this diameter, while the other half are smaller; hence this is the Mass median aerodynamic diameter (MMAD).

Fine particle dose = mass of fine particles on stages 2 through 7

$$\text{Fine particle fraction (FPF)} = \frac{\text{Fine particle dose}}{\text{Initial particle mass}} \times 100$$

$$\text{Emitted dose} = \frac{\text{Total particle mass on all stages}}{\text{Initial particle mass}} \times 100$$

Finally, an online MMAD calculator was used to calculate the mass median aerodynamic diameter (MMAD) and geometric standard deviation.

##### 2.4.3. In vitro studies on drug release of the optimized microspheres

DMC was released from O-DMC-MP at pH level 7.4 (phosphate buffer) and has been studied to determine the drug release profile (Schafroth et al., 2012). In short, 25 mg of O-DMC-MP was put into 500 mL of dissolution medium that was kept at 37 ± 0.5 °C at 100 rpm. Samples of 1 mL were taken at regular intervals and examined by HPLC (as mentioned in section 2.3.2) to determine how much drug was in the solution. After each withdrawal, the same amount of fresh dissolution medium was added to keep the initial volume of the dissolution medium the same (D'Souza and DeLuca, 2005).

##### 2.4.4. Cytotoxicity

To determine if O-DMC-MP was harmful to HUVEC, H1299, and A549 cells, the MTT test was utilized. A549 and H1299 cells were placed onto clear, flat-bottomed 96-well plates at a density of 5,000 or 10,000 cells per well, respectively, and were then incubated at 37 °C for 24 h until they were roughly 80% full. The cells were placed in 200 μL of growth media with MP at seven different concentrations after being rinsed with PBS at 37 °C (Nair et al., 2021). We employed cells allowed to increase in growth medium as a negative control. 5 μL of 5 mg/mL MTT reagent was given to the cells after they had been cultured with the various formulae for the required 24 h. For formazan crystals to form, the cells were treated for 3.5 h (HUVEC) or 3 h (H1299 and A549) at 37 °C. After removing the medium, 150 μL of DMSO was added to each well to dissolve the formazan crystals and disintegrate the cells. To account for the background of the cells, the absorbance was measured at 540 nm and 650 nm using a Synergy MX plate reader (Bio-Tek, Winooski, VT, USA). The equation was used to calculate cell viability (Agnoletti et al., 2020).

$$\text{Cell viability (\%)} = \frac{A \text{ treated cells @ 540nm} - A \text{ treated cells @ 650nm}}{A \text{ untreated cells @ 540nm} - A \text{ untreated cells @ 650nm}} \times 100$$

The absorbances at 540 nm of the wells holding the test sample (A treated cells @540 nm) and the background absorbances at 650 nm (A untreated cells @650 nm) are given. To get IC50 values, we use GraphPad Prism 8 to fit the data to a nonlinear regression model with a varying slope. These values show how much the treatment stopped 50% of the dehydrogenase in the cells.

##### 2.4.5. Stability studies

Stability studies were performed to confirm the integrity and stability of the optimize formulation. So that the stability process would meet the standards set by ICH, it was made. The O-DMC-MP was put into capsules, kept in glass vials, and put in a stability room at different temperatures and levels of humidity: 4 °C/ambient RH, and 40 °C/75% RH. Over up to 3 months, PS, EE, and physical characteristics were evaluated at various intervals.

#### 2.5. In vivo studies

##### Animals.

Male Swiss albino mice were six weeks old and weighing between 20 and 25 g were obtained from the Biogen Laboratory Animal Facility in Bengaluru, India. The animals were kept in an ordinary place with a temperature of 25 °C and a humidity of 50%. They could get food and water from the lab for free. The Sri Adichunchanagiri College of Pharmacy's Institutional Animal Ethical Committee reviewed the experiment plan and gave the clearance. (No. SACCP/IAEC-04/2023).

### 2.5.1. Hemocompatibility

The Evans et al.-inspired hemolysis process was used to test how well the formulation interacts with the systemic circulation. To get red blood cells (RBC), blood from the animal was put in a K2-EDTA-coated Vacutainer and spun at 700 g for five minutes at room temperature (Evans et al., 2013). The RBC were removed from the plasma, centrifuged at 700g for five minutes at room temperature, and then gently washed four times with 150 mM NaCl in ultrapure water and four times with PBS. The RBC were diluted to 3% (w/v) in PBS, and 100  $\mu$ L of 1 mg/mL, 2 mg/mL and 4 mg/mL amounts of O-DMC-MP in PBS were added to 100  $\mu$ L of this mixture. Triton<sup>TM</sup> X-100 2% (v/v) and PBS were used as positive and negative controls, respectively. The Eppendorf<sup>®</sup> tubes were kept at 37 °C on a rotating shaker for one hour. Then, the RBC were separated by spinning the tubes at 700g at room temperature for five minutes. The hemoglobin absorbance at 450 nm was measured using a BioTek Synergy MX plate reader after the supernatant was plated into a round-bottom 96-well plate (Falcon<sup>TM</sup>, Corning, NY, USA). The following formula determined the proportion of hemolysis.

$$\text{Hemolysis (\%)} = \frac{(\text{A sample} - \text{A negative control})}{(\text{A positive control} - \text{A negative control})} \times 100$$

where A sample is the absorbance of the supernatant from the RBC incubated with the different concentrations of the formulations, A negative control is the absorbance of the supernatant from the RBC incubated with PBS, and A positive control is the absorbance of the supernatant from the RBC incubated with Triton<sup>TM</sup> X-100.

### 2.5.2. Pharmacokinetic and organ biodistribution study

For the pharmacokinetic study, random assignment put Swiss white mice into two groups. The control group got free DMC, while the treatment group got an optimized formula. Dry powder fumes were breathed into the lungs with a device that help to breathe through their nose (Harsha et al., 2015a; Luo et al., 2016; Satyavert et al., 2021). Every animal got 10 mg/kg of DMC. At 0.5, 1.5, 3, 6, 9, 12, 24, and 36 h, 200  $\mu$ L of blood from each mouse was taken and put into micro-tubes treated with heparin. The tubes were spun at 5000  $\times$  g rpm to split the plasma for 20 min. The DMC was then taken out by mixing 100  $\mu$ L of the plasma samples with 100  $\mu$ L of acetonitrile in a swirl for 30 s. The samples were then put through a 0.22  $\mu$ m membrane filter, and an HPLC device was used to measure how much drug was in each sample.

The pharmacokinetic measures of DMC were calculated using the PKSolver 2.0 software.

After taking blood samples at certain times, the mice were put to sleep, and their lungs, liver, heart, kidneys, and spleens were cut open to study biodistribution (Kaur et al., 2008; Sharma et al., 2001). The organs were rinsed with cold phosphate buffer saltwater (pH 7.4), dried, weighed, and mixed for one minute at 10,000  $\times$  g rpm in an ice bath. 100  $\mu$ L of acetonitrile was combined with 100  $\mu$ L of each sample, and the mixture was shaken for 5 min to get the DMC out. After 10 min of 10,000 g/rpm centrifuging, the supernatants were divided, and the HPLC system was used to look for DMC.

### 2.6. Statistical analysis

Mean and SD was calculated for each response. The single Student's *t*-test (SPSS software version 16; SPSS Inc., Chicago, IL, USA) was used to determine statistical parameters. A p-value of less than 0.05 showed a significant change.

## 3. Results and discussion

### 3.1. Optimization of preparation of DMC-MP

Design Expert 11 used a 3-factor, 3-level Box-Behnken design (Version 11.0, Stat-Ease Inc.) to look at quadratic response surfaces. Table 2 represents the results of 17 runs and how the different trails were planned. Three-dimensional plots are known for demonstrating the effect of selected factors interaction of on the chosen responses.

The quadratic model was selected for all solutions based on the Type-I sequential sum of squares and the fit summary. We selected the model based on the F-value, the p-value, and the R<sup>2</sup> value. In addition, the quadratic model has the lowest p-value (0.0001) of any polynomial order (Table 3).

All the above ANOVA coefficients can be used to determine the significant factors and their magnitude of impact. Contour plots and 3D response surface graphs (RSG) are needed to describe the main effects of selected factors and their interaction [Fig. 2]. PS was found to be less when there was a decline in liquid paraffin and glutaraldehyde concentrations. Increased concentrations of both factors can shoot up the EE.

Using the desire function [D], different models that came out of an experiment can be made as good as they can be (Naveen et al.,

**Table 2**  
Observed responses in Box-Behnken design for developing and optimizing DMC-MP.

Std	Run	Factor 1 A:Liquid paraffin ml	Factor 2 B:Glutaraldehyde %	Factor 3 C:Span-80 g	Response 1 PS um	Response 2 EE %
1	17	10	10	0.5	4.5	35.5
9	3	20	10	0.25	6.5	41.5
11	9	20	10	0.75	7.2	48.2
2	8	30	10	0.5	7.6	49.2
5	7	10	25	0.25	7.9	51.2
7	11	10	25	0.75	7.9	74.58
13	5	20	25	0.5	8.4	75.1
14	6	20	25	0.5	8.3	73.5
17	10	20	25	0.5	8.1	76.8
16	13	20	25	0.5	7.9	79.8
15	16	20	25	0.5	8.3	76.2
6	2	30	25	0.25	9.8	82.25
8	4	30	25	0.75	11.5	86.21
3	15	10	40	0.5	12.9	71.25
12	1	20	40	0.75	13.5	92.75
10	14	20	40	0.25	14.2	89.25
4	12	30	40	0.5	13.2	95.87

**Table 3**  
Model statistical summary.

Response	Models	R <sup>2</sup>	Adju.R <sup>2</sup>	Pred.R <sup>2</sup>	Adequate precision	Sequential p-value	CV (%)	Remarks
EE	Linear	0.8796	0.8519	0.7809	---	<0.0001	4.58	Suggested
	2 FI	0.9028	0.8445	0.6373	---	0.5247		
	Quadratic	<b>0.9866</b>	<b>0.9695</b>	<b>0.8437</b>	25.7961	<b>0.0021</b>		
PS	Cubic	0.9960	0.9841	---	---	0.1490	4.22	Suggested
	Linear	0.8787	0.8507	0.7926	---	<0.0001		
	2 FI	0.9044	0.8471	0.7027	---	0.4757		
	Quadratic	<b>0.9913</b>	<b>0.9801</b>	<b>0.8795</b>	32.4773	<b>0.0005</b>		
	Cubic	0.9987	0.9948	---	---	0.0396		

The way the experiment was set up suggested that EE could be changed by the combined effect of all the essential factors, with B effects being the most critical [Table 4].  
 PS = 8.2 + 1.1125 A + 3.5B + 0.2125C - 0.7 AB + 0.425 AC - 0.35BC + 0.1375 A<sup>2</sup> + 1.2125B<sup>2</sup> + 0.9375 C<sup>2</sup>.  
 EE = 76.28 + 10.125 A + 21.84B + 4.6925C + 2.73 AB - 4.855 AC - 0.8 BC - 3.845 A<sup>2</sup> - 9.48 B<sup>2</sup> + 1.125 C<sup>2</sup>.

**Table 4**  
ANOVA coefficients table.

	Intercept	A	B	C	AB	AC	BC	A <sup>2</sup>	B <sup>2</sup>	C <sup>2</sup>
<b>PS</b>	8.2	<b>1.1125</b>	<b>3.5</b>	0.2125	<b>-0.7</b>	0.425	-0.35	0.1375	<b>1.2125</b>	<b>0.9375</b>
<b>p-values</b>		<b>&lt;0.0001</b>	<b>&lt;0.0001</b>	0.1685	<b>0.0090</b>	0.0665	0.1169	0.4944	<b>0.0004</b>	<b>0.0017</b>
<b>EE</b>	76.28	<b>10.125</b>	<b>21.84</b>	<b>4.6925</b>	2.73	<b>-4.855</b>	-0.8	<b>-3.845</b>	<b>-9.48</b>	1.125
<b>p-values</b>		<b>&lt;0.0001</b>	<b>&lt;0.0001</b>	<b>0.0045</b>	0.1349	<b>0.0198</b>	0.6357	<b>0.0446</b>	<b>0.0005</b>	0.4981

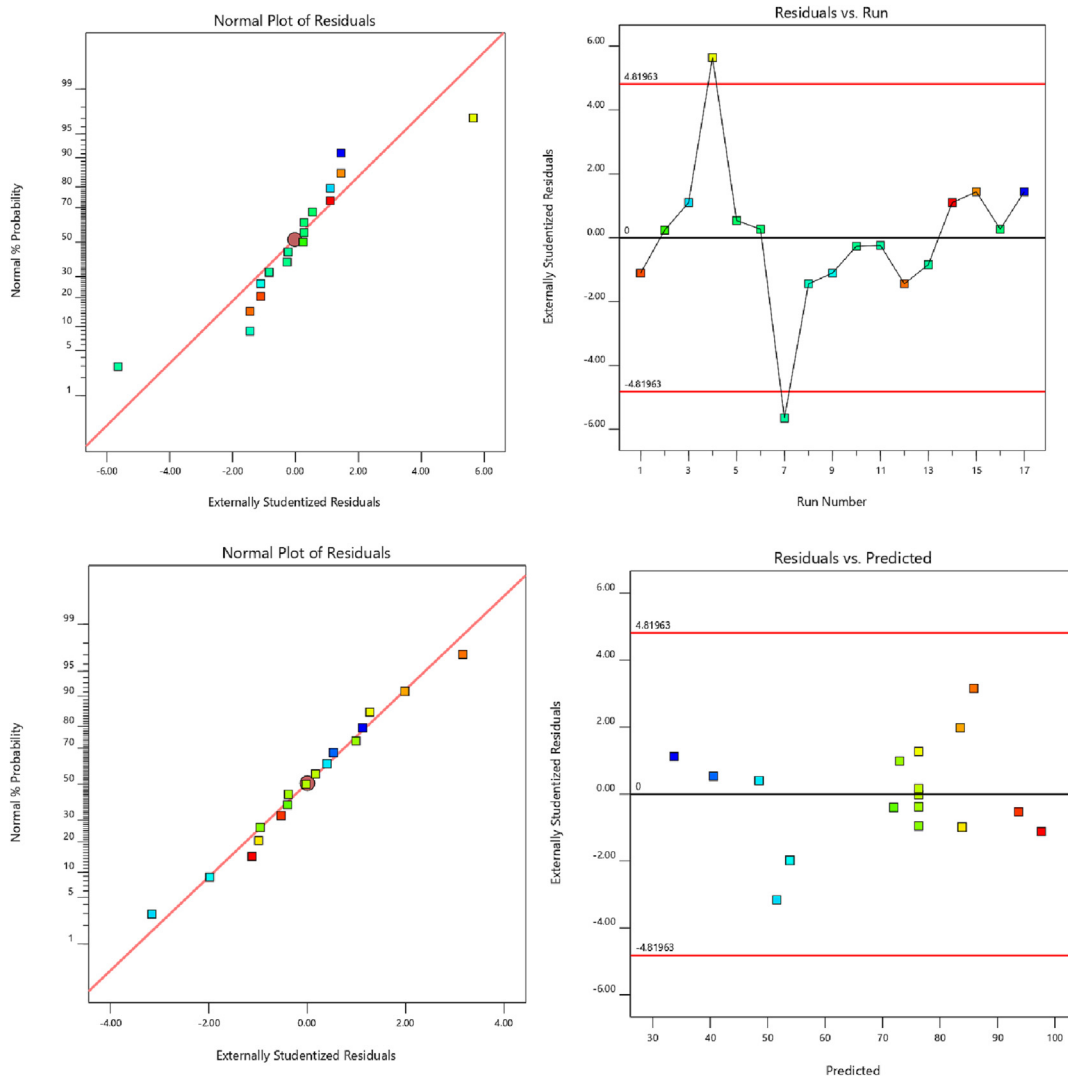


**Fig. 1.** The normal plot for residuals and residuals vs. run for PS and EE.

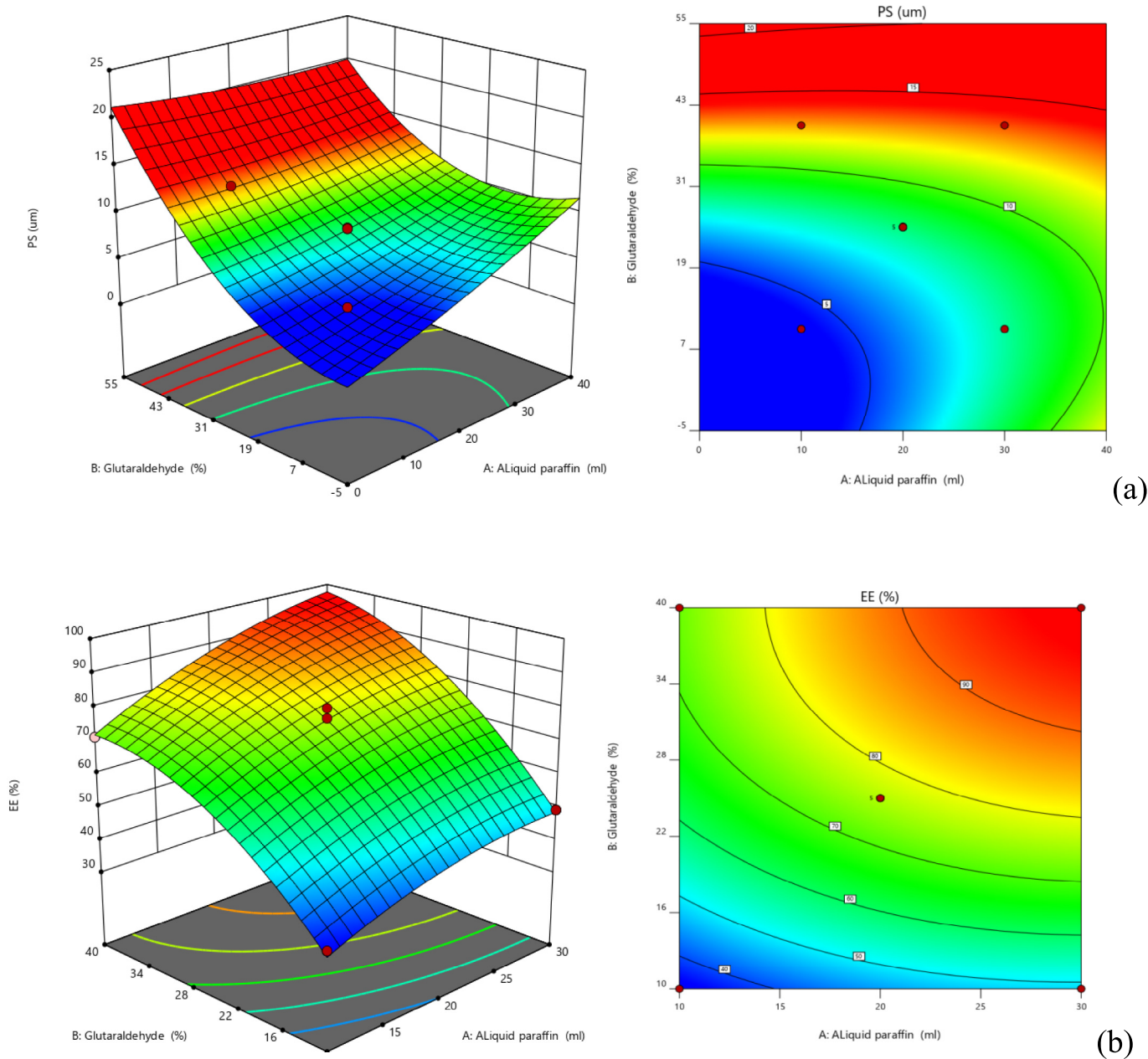


Fig. 2. Contour and 3-D response surface graphs for a) PS and b) EE.

2017; Salatin and Jelvehgari, 2021). A minimum PS and maximum EE were set for each answer, among other boundaries, to make the overlay graph. The design space had all of the things that were picked. At the best densities of the independent variables, all the answers combined desirability plots had the highest D value of 0.897, and the most critical answers were stacked on top of each other in the contour plot [Fig. 3-a].

Based on this method, a formulation that meets the conditions of the ideal formulation can be made with 19.61 mL of liquid paraffin, 24.26% of glutaraldehyde, and 0.58 gm of span-80. So, the PS is expected to be 8.16  $\mu\text{m}$ , and the EE can be 76.55%. The optimized formulation of O-DMC-MP was made and tested using these predicted ideal ratios to see if it was better. To back up how the experience was set up, the experiment's results were compared to the numbers from the theory. It was found that the results were having the difference of less than 3%. The particle size distribution of O-DMC-MP has been portrayed in Fig. 3-b. The particle size of O-DMC-MP met the results of the desirability test, and the zeta potential was found to be

−38.5 mV, which shows that the composition is stable. A UV-Vis spectrophotometer was used to figure out the EE and DL readings after the drug molecules were dissolved in methanol in a certain way. DMC's EE was found to be 76.55%, and her DL to be 65.84%. Obviously, the MP that was made can be used to make novel systems that can reach to lungs and have a high EE and good DL.

### 3.2. SEM

The SEM pictures (Fig. 4) showed that many microspheres were the same size, had smooth surfaces, and didn't stick together.

### 3.3. Dispersion

Most of the time, particles with an aerodynamic width of 1 to 10  $\mu\text{m}$  can quickly settle in the deep part of the lungs (Evans et al., 2013). Table 5 shows the dispersion parameters of optimized formulation.

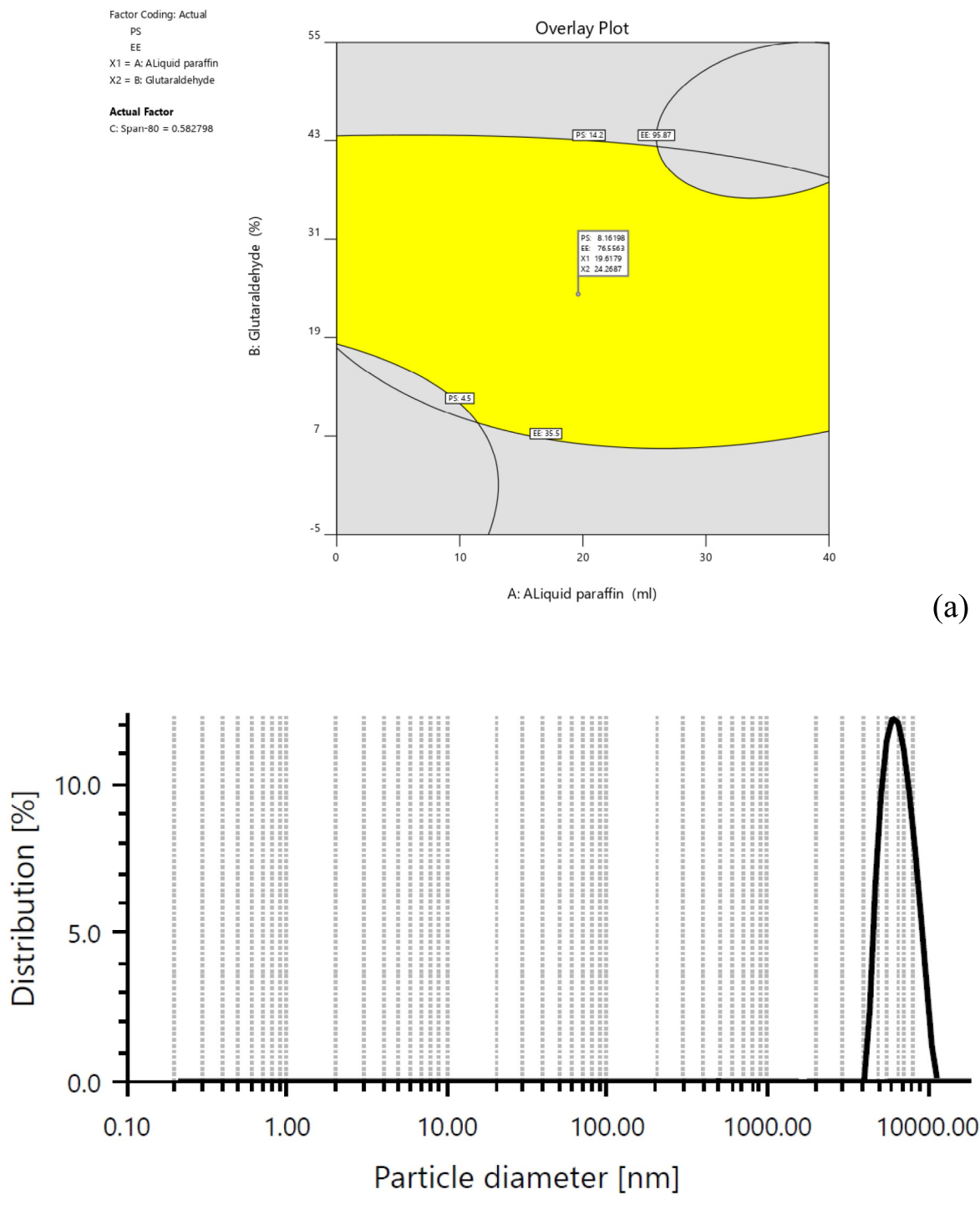


Fig. 3. A) overlay plot and b) ps distribution of optimized formulation.

### 3.4. Drug release

Fig. 5 shows the release of DMC from DMC suspension and optimized formulation concerning different intervals of time.

### 3.5. Cytotoxic study

Fig. 6A–C shows that for HUVEC, A549, and H1299, the IC50 values for MP that weren't loaded were 1.2 mg/mL, 4.8 mg/mL, and

1.8 mg/mL, respectively. This is in line with what other studies have found.

### 3.6. Stability studies

The stability of the optimized formulation during storage is a critical factor that affects the physicochemical properties of powder MP that are meant to be inhaled, such as their look, particle size, how well they trap drugs, and how much drug they can hold. Table 6 lists all of the things that happen when O-DMC-MP is

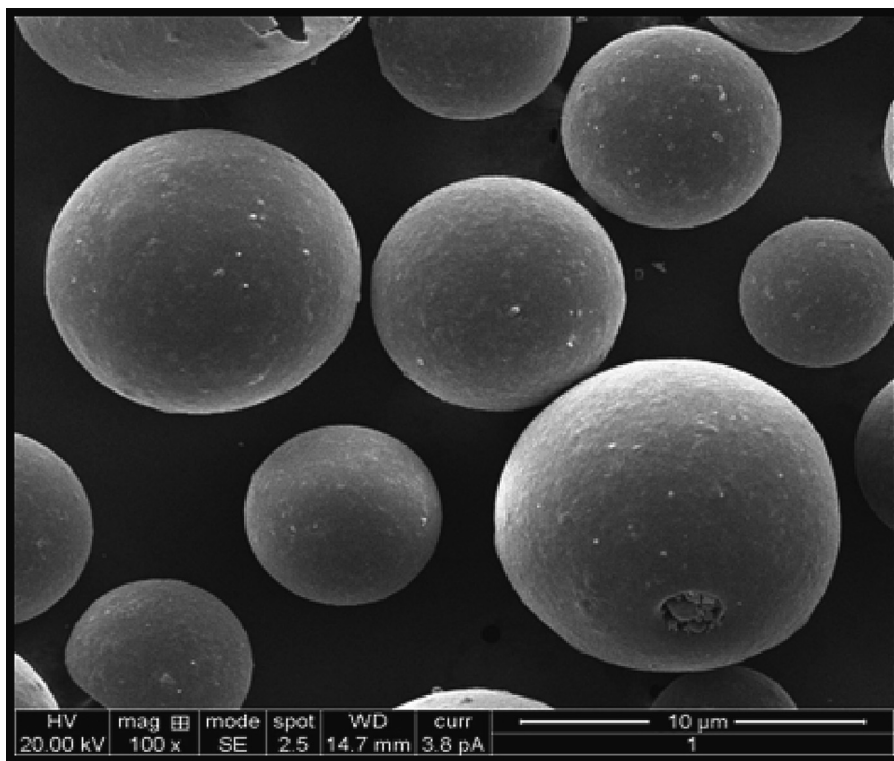


Fig. 4. SEM image of O-DMC-MP.

**Table 5**  
Aerodynamic parameters of O-DMC-MP.

Parameters	O-DMC-MP
MMAD ( $\mu\text{m}$ )	$8.46 \pm 1.45$
Geometric standard deviation	$1.89 \pm 1.09$
Recovered dose ( $\mu\text{g}$ )	$90.45 \pm 1.89$
Emitted dose ( $\mu\text{g}$ )	$81.48 \pm 2.15$
Fine particle dose ( $\mu\text{g}$ )	$65.06 \pm 2.08$
Fine particle fraction (%) (FPF)	$77.69 \pm 1.26$

stored. Whether the temperature was slowed down or sped up, none of the factors changed much over the three-month storage time ( $p$  greater than 0.05). These results show that the planned formulations are stable over time and in different storage situations.

3.7. Hemolytic study

Fig. 7 demonstrates that neither the formulation (6 mg/mL) nor the free DMC (0.6 mg/mL) generated more than 0.6% hemolysis at

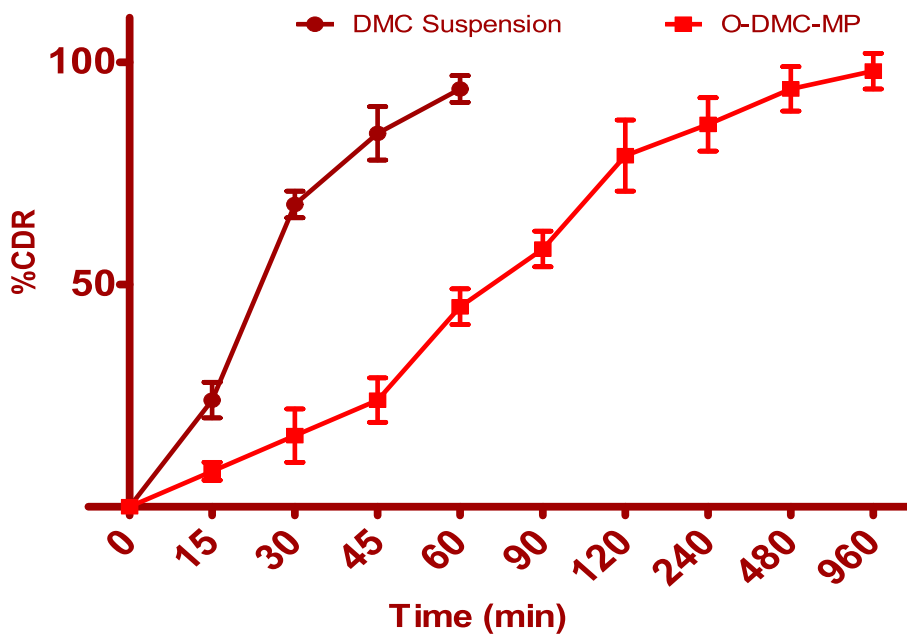


Fig. 5. In vitro drug release profile of Pure DMC suspension and O-DMC-MP.



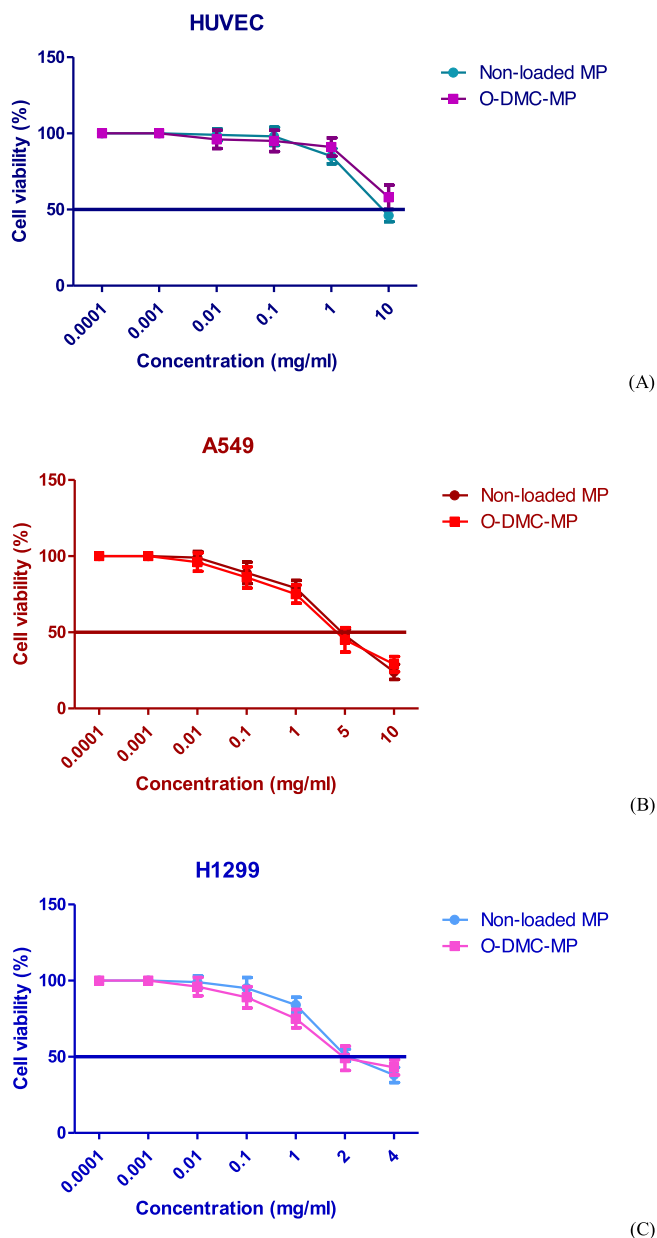


Fig. 6. Cell viability studies on A) HUVEC, B) A549 and C) H1299 cell lines.

concentrations three times the dose provided *in vivo* for the components.

3.8. Pharmacokinetic, biodistribution and targeting efficiency

After giving plain drugs or drug-loaded microspheres through the lungs, the pharmacokinetics of DMC in living things were looked at. Fig. 8-A & B shows how the amount of DMC in the blood

and lungs changes over time after breathing in plain DMC or O-DMC-MP.

3.9. Biodistribution study

Fig. 9 shows that both plain DMC and O-DMC-MP quickly and preferentially accumulated in the lung after pulmonary administration, with  $79.14 \pm 1.24\%$  and  $87.25 \pm 5.89\%$  of the breathed dose in the lung within 30 min.

4. Discussion

The standard plot of residuals showed that all of the models that were chosen were significant. In this case, the graph that can be seen will be enough, so the suggested statistical program won't be needed. The proposed model can be accepted statistically because all studentized residuals for the chosen responses were more evenly spread along a straight line (Mallamma et al., 2014; Raghavendra Naveen et al., 2023). The experimental run and residuals are compared in Fig. 1 to identify the confounding variables. A random trend was seen within the allowable range, indicating the presence of a time-coupled variable.

For EE, there is less than a 0.2 difference between the Predicted R2 of 0.9695 and the Adjusted R2 of 0.8437. By Adeq Precision, the signal-to-noise ratio is measured. The ideal ratio is more significant than four. A strong signal is indicated by the ratio of 25.7961. Navigation in the design area is made more accessible by this method. The PS [0.9801, 0.8795, and 32.4773] results were similar (Rizg et al., 2022; Rowley et al., 1999). The coefficient of variation (CV) value demonstrates that the repeatability of the experiments reflects the clarity of the technique while also guaranteeing the correctness of the results. Consistency and correctness of the design were guaranteed because the desired CV value was less than the mandated (CV10 percent) (4.58% for EE and 4.22% for PS). Lack of Fit is another parameter that assesses how well the model fits the data. The ANOVA findings show that the Lack of Fit is non-significant ( $p > 0.05$ ), indicating that the selected design is appropriate. The quantitative effects of particular variables on responses were investigated using an ANOVA. To create polynomial equations, multiple regression was applied to the data that had been gathered. All models were statistically significant, as shown by the model F-values of 88.57 and 52.24 (Hooda et al., 2012; Popoola, 2019). The model terms A, B, AB, and all quadratic terms are significant for PS. How the experiment was set up suggested that i could change PS) the effect of factors A, B working against factor AB, and ii) the impact of all the other essential factors working together, with B having the most substantial effect of all the terms.

Enhanced imaging was used to determine the best formulation's shape or morphology utilizing a method like SEM. The SEM pictures (Fig. 4) showed that many microspheres were the same size, had smooth surfaces, and didn't stick together. This is because the right excipients were used. Overall, the data on particle size definition is suitable for passive targeting of the lungs and is related to the size distribution of particles.

Table 6 Stability studies of O-DMC-MP.

Parameter	Initial	4 ± 1 °C (1 Month)	4 ± 1 °C (3 Months)	40 ± 2 °C & 75 ± 5% RH (1 Month)	40 ± 2 °C & 75 ± 5% RH (3 Months)
PS (um)	8.26	8.31	8.35	8.78	8.96
EE (%)	76.55	76.04	75.43	75.13	75.46
Physical characteristics	Complies	Complies	Complies	Complies	Complies

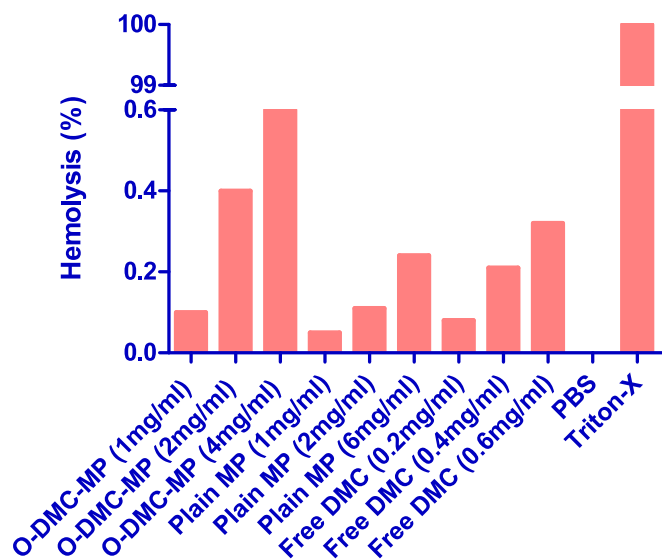


Fig. 7. Hemolysis study.

The MMAD of the optimization mix was found to be  $8.46 \pm 1.45 \mu\text{m}$ . Also, there were a lot of finer particles in the final formulation. These results show that making MP with O-DMC-MP is better. Also, most of the DMC-loaded microspheres were kept in the cascade impactor at stages 5 and 6, which had smaller aerodynamic cut-off sizes because their MMAD was smaller and their FPF was higher. All of these studies show that the planned formulation goes deep into the lungs.

More than 75% of the regular DMC was released in less than 45 min, as shown in Fig. 5. Only 24% of the drug was released from the microsphere version after 45 min, much less than the plain drug solution. As an additional note, drug-loaded O-DMC-MP microspheres exhibited a two-phase release pattern, with a rapid burst release (79%) in the first two hours and a continuous release for up to 16 h. DMC-filled microspheres may experience an initial burst of drug release as drug molecules released from the microspheres outer layers. The sluggish distribution of pharmaceuticals from the microspheres core, the gradual erosion/degradation of the polymeric matrix, or some combination of the two may be

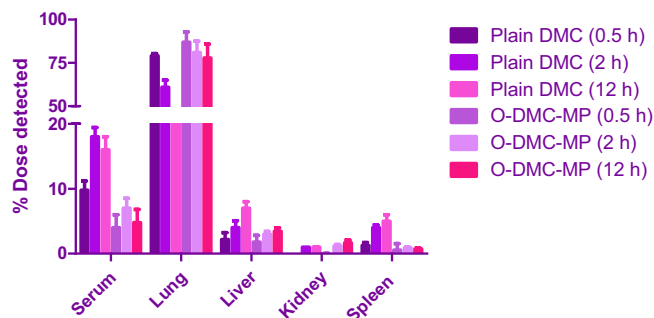


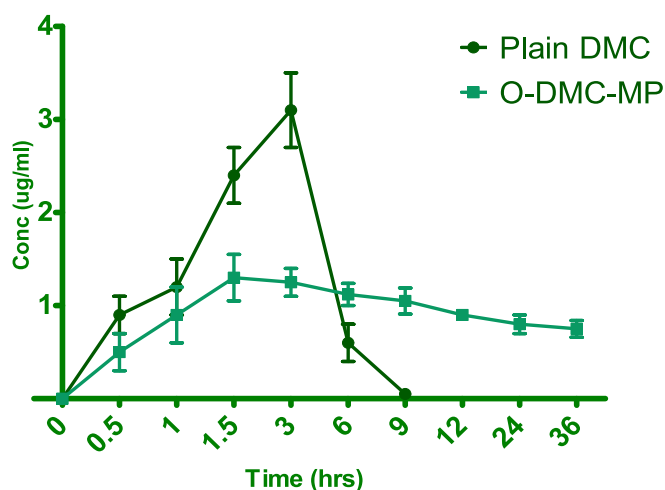
Fig. 9. Biodistribution study of plain DMC and O-DMC-MP.

responsible for the comparatively slow release of drugs from the microspheres. Note that the way DMC was released from microspheres in test tubes didn't change much at any of the other tested pH levels [data not shown].

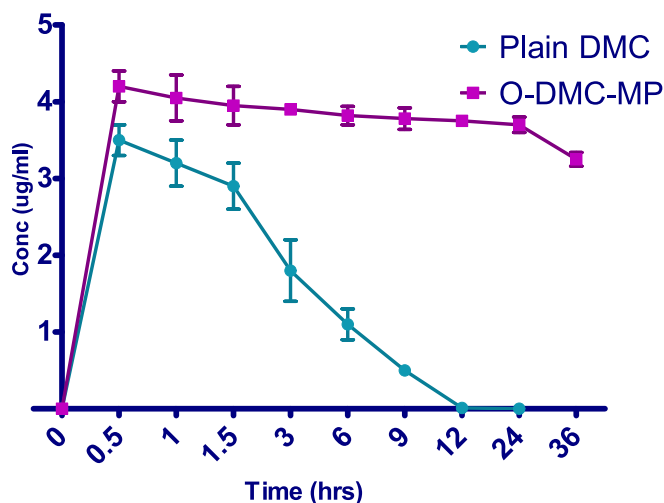
To find out the toxicity of O-DMC-MP to cells, endothelial (HUVEC), alveolar lung epithelial (A549), and human lung epithelial (H1299) cell lines were used. The MP with DMC was just as bad for all three cell lines, with IC50 values of 1.8–2.1 mg/mL for HUVEC, 4.0–5.5 mg/mL for A549, and 1.4–2.4 mg/mL for H1299. The cytotoxicity of O-DMC-MP was not depend on the amount of DMC released in initial timings, since the same amounts of free DMC did not cause cytotoxicity (Fornaguera et al., 2015; Gaspar et al., 2019). These results show that adding chitosan and glutaraldehyde to the DMC doesn't change the cytotoxicity much, which is similar to what Gaspar et al. found when they tested lung Calu-3 cells.

Even when a drug is given through the lungs, it is essential to assure its fate in systemic circulation. At the concentrations tested (1–6 mg/ml), plain MP, O-DMC-MP, and free DMC did not kill erythrocytes. The results show that DMC-MP is safe to in treating ARDS. Studies done in the past show that chitosan nanoparticles up to 3 mg/mL did not cause hemolysis. But as far as the writers know, there have been no reports of higher concentrations.

Fig. 8 A shows that compared to O-DMC-MP, the blood concentration of plain DMC rose quickly after inhaling the drug and hit a much higher peak soon after. The quick absorption of drugs by the lungs' alveoli, which have many blood vessels, could be to the pos-



(a)



(b)

Fig. 8. Pharmacokinetic profile of plain DMC and O-DMC-MP in a) plasma and b) lung following pulmonary inhalation.

sible reason for the relatively higher plasma drug levels for plain medicines after pulmonary administration (Powers, 2022). On the other hand, the smaller amount of DMC in the blood after inhaling drug-loaded microspheres may be because the drug is released more slowly from the microspheres. This would make it take longer for the drug to be absorbed. Fig. 8B shows the lung concentration of DMC over time after it was taken in as either plain DMC or O-DMC-MP. As soon as both plain DMC and O-DMC-MP were given, it was clear that the lungs had more of the drug.

Most importantly, O-DMC-MP showed that it could keep drug concentrations high and DMC in the lungs for up to 24 h after microspheres were breathed. On the other hand, there was a big drop in the amount of plain DMC in the lungs right after living the drug. The quick movement of plain DMC from the pleural cavity to the systemic circulation could be to blame for the drop in free drug concentration in the lungs (Patton et al., 2004). This is shown by simultaneously raising the drug amount in the plasma.

The success of focused drug therapy rests on how well the drug is distributed in the body and gets to where it works. So, after plain DMC and O-DMC-MP were given through the lungs, their spread through the body was tracked. With plain DMC, on the other hand, the amount of drug in the lungs slowly decreased over time. After 30 min, the amount of plain DMC in the body dropped from 79.141.24% to 41.256.24%. Blood, liver, kidneys, and spleen have all been found to have about 12% of DMC.

On the other hand, O-DMC-MP desposited DMC in lung tissue for longer and in higher amounts. Even after 12 h, 77.85% of the amount that was inhaled through microspheres was still in the lung tissue. More than 80% of the drug was found in the lungs in the first few hours, which is what was expected based on how the drug works. Also, when nanoparticles were inhaled, the amount of DMC that built up in the spleen, liver, and kidneys was much lower than when plain DMC was inhaled. This showed that pulmonary microsphere delivery cut down on the amount of drug that went to organs other than the lungs. These studies show that microspheres are an excellent way to keep a drug's (DMC) pharmacological activity inside them. This is probably done by making it harder for the drug to leave the lungs through the alveoli and by making it stay in the body longer. This, in turn, would make it possible for the right amount of drug to be released at the spot of action.

## 5. Conclusion

This project aimed to make dry powder MP of dexamethasone (DMC) that contained chitosan and could be taken in. By emulsion crosslinking, DMC-MP was prepared. The box-Behnken design was used to find the suitable PS and EE for the best microspheres to target alveolar macrophages through non-invasive pulmonary transport. Based on the desirability approach, a formulation containing 19.61 mL of liquid paraffin, 24.26% of glutaraldehyde, and 0.58 gm of span-80 can meet the prerequisites of the formulation. Also, the optimized formulation had an ideal average aerodynamic diameter and a fine particle fraction, which showed they were suitable for aerosolization. Also, as evident from the biodistribution study, DMC-loaded MP kept a relatively high drug dose in the lungs for a longer time and helped the drug stay there longer. Inhaling DMC-loaded microspheres could be an excellent way to treat acute respiratory distress syndrome because it makes DMC more effective as a drug while reducing its side effects in effectively treating ARDS.

## Funding

Not applicable

## Declaration of Competing Interest

The authors declare that they have no known competing financial interests or personal relationships that could have appeared to influence the work reported in this paper.

## Acknowledgment

The authors would like to thank the Adichunchanagiri University, for providing the facilities to conduct these studies.

## References

- Abraham, S.M., Lawrence, T., Kleiman, A., Warden, P., Medghalchi, M., Tuckermann, J., Saklatvala, J., Clark, A.R., 2006. Antiinflammatory effects of dexamethasone are partly dependent on induction of dual specificity phosphatase 1. *J. Exp. Med.* 203. <https://doi.org/10.1084/jem.20060336>.
- Agnoletti, M., Agnoletti, M., Rodríguez-Rodríguez, C., Rodríguez-Rodríguez, C., Klodzińska, S.N., Esposito, T.V.F., Esposito, T.V.F., Saatchi, K., Mørck Nielsen, H., Häfeli, U.O., Häfeli, U.O., 2020. Monosized polymeric microspheres designed for passive lung targeting: biodistribution and pharmacokinetics after intravenous administration. *ACS Nano* 14. <https://doi.org/10.1021/acsnano.9b09773>.
- Aldawsari, H.M., Naveen, N.R., Alhakamy, N.A., Goudanavar, P.S., Rao, G.K., Budha, R., Nair, A.B., Badr-Eldin, S.M., 2022. Compression-coated pulsatile chronomodulated therapeutic system: QbD assisted optimization. *Drug Deliv.* 29, 2258–2268. <https://doi.org/10.1080/10717544.2022.2094500>.
- Anandharamkrishnan, C., Rielly, C.D., Stapley, A.G.F., 2007. Effects of process variables on the denaturation of whey proteins during spray drying. *Drying Technol.* 25. <https://doi.org/10.1080/07373930701370175>.
- Baldinger, A., Clerdent, L., Rantanen, J., Yang, M., Grohgan, H., 2012. Quality by design approach in the optimization of the spray-drying process. *Pharm. Dev. Technol.* 17. <https://doi.org/10.3109/10837450.2010.550623>.
- Bleecker, E.R., Menzies-Gow, A.N., Price, D.B., Bourdin, A., Sweet, S., Martin, A.L., Alacqua, M., Tran, T.N., 2020. Systematic literature review of systemic corticosteroid use for asthma management. *Am. J. Respir. Crit. Care Med.* <https://doi.org/10.1164/rccm.201904-0903SO>.
- Brugnera, M., Vicario-De-la-torre, M., Andrés-Guerrero, V., Bravo-Osuna, I., Molina-Martinez, I.T., Herrero-Vanrell, R., 2022. Validation of a rapid and easy-to-apply method to simultaneously quantify co-loaded dexamethasone and melatonin PLGA microspheres by HPLC-UV: encapsulation efficiency and in vitro release. *Pharmaceutics* 14. <https://doi.org/10.3390/PHARMACEUTICS14020288/S1>.
- Charoo, N.A., Shamsher, A.A.A., Zidan, A.S., Rahman, Z., 2012. Quality by design approach for formulation development: a case study of dispersible tablets. *Int. J. Pharm.* 423. <https://doi.org/10.1016/j.ijpharm.2011.12.024>.
- Cipolla, D., Shekunov, B., Blanchard, J., Hickey, A., 2014. Lipid-based carriers for pulmonary products: preclinical development and case studies in humans. *Adv. Drug Deliv. Rev.* <https://doi.org/10.1016/j.addr.2014.05.001>.
- D'Souza, S.S., DeLuca, P.P., 2005. Development of a dialysis in vitro release method for biodegradable microspheres. *AAPS PharmSciTech* 6. <https://doi.org/10.1208/pt060242>.
- Dolma Gurung, B., Kakar, S., 2020. An overview on microspheres. *Gurung and Kakar Int. J. Health Clin. Res.* 3.
- Evans, B.C., Nelson, C.E., Yu, S.S., Beavers, K.R., Kim, A.J., Li, H., Nelson, H.M., Giorgio, T.D., Duvall, C.L., 2013. Ex vivo red blood cell hemolysis assay for the evaluation of pH-responsive endosomolytic agents for cytosolic delivery of biomacromolecular drugs. *J. Vis. Exp.* <https://doi.org/10.3791/50166-v>.
- Ezhilarasi, P.N., Indrani, D., Jena, B.S., Anandharamkrishnan, C., 2014. Microencapsulation of Garcinia fruit extract by spray drying and its effect on bread quality. *J. Sci. Food Agric.* 94. <https://doi.org/10.1002/jsfa.6378>.
- Ferguson, N.D., Fan, E., Camporota, L., Antonelli, M., Anzueto, A., Beale, R., Brochard, L., Brower, R., Esteban, A., Gattinoni, L., Rhodes, A., Slutsky, A.S., Vincent, J.L., Rubenfeld, G.D., Taylor Thompson, B., Marco Ranieri, V., 2012. The Berlin definition of ARDS: an expanded rationale, justification, and supplementary material. *Intensive Care Med.* 38. <https://doi.org/10.1007/s00134-012-2682-1>.
- Fornaguera, C., Calderó, G., Mitjans, M., Vinardell, M.P., Solans, C., Vauthier, C., 2015. Interactions of PLGA nanoparticles with blood components: Protein adsorption, coagulation, activation of the complement system and hemolysis studies. *Nanoscale* 7. <https://doi.org/10.1039/c5nr00733j>.
- Gaspar, M.C., Pais, A.A.C.C., Sousa, J.J.S., Brillault, J., Olivier, J.C., 2019. Development of levofloxacin-loaded PLGA microspheres of suitable properties for sustained pulmonary release. *Int. J. Pharm.* 556. <https://doi.org/10.1016/j.ijpharm.2018.12.005>.
- Hagbani, T.A., Vishwa, B., Abu Lila, A.S., Alotaibi, H.F., Khafagy, E.S., Moin, A., Gowda, D.V., 2022. Pulmonary targeting of levofloxacin using microsphere-based dry powder inhalation. *Pharmaceutics* 15, 560. <https://doi.org/10.3390/PH15050560/S1>.
- Harsha, S., Al-Dhubiab, B.E., Nair, A.B., Al-Khars, M., Al-Hassan, M., Rajan, R., Attimarad, M., Venugopala, K.N., Asif, A.H., 2015a. Novel drying technology of microsphere and its evaluation for targeted drug delivery for lungs. *Drying Technol.* 33. <https://doi.org/10.1080/07373937.2014.963202>.

- Harsha, S.N., Aldhubiab, B.E., Nair, A.B., Alhaider, I.A., Attimmarad, M., Venugopala, K. N., Srinivasan, S., Gangadhar, N., Asif, A.H., 2015b. Nanoparticle formulation by Büchi B-90 Nano Spray Dryer for oral mucoadhesion. *Drug Des. Devel. Ther.* 9, 273. <https://doi.org/10.2147/DDDT.S66654>.
- Heda, A., Kathiriya, J., Gadade, D., Puranik, P., 2011. Development and Validation of RP-HPLC Method for Simultaneous Determination of Granisetron and Dexamethasone. *Indian J. Pharm. Sci.* 73, 696. <https://doi.org/10.4103/0250-474X.100255>.
- Hooda, A., Nanda, A., Jain, M., Kumar, V., Rathee, P., 2012. Optimization and evaluation of gastroretentive ranitidine HCl microspheres by using design expert software. *Int. J. Biol. Macromol.* 51. <https://doi.org/10.1016/j.ijbiomac.2012.07.030>.
- Hosny, K.M., Naveen, N.R., Kurakula, M., Sindi, A.M., Sabei, F.Y., Fatease, A.A., Jali, A. M., Alharbi, W.S., Mushtaq, R.Y., Felemban, M., 2022. Design and development of neomycin sulfate gel loaded with solid lipid nanoparticles for buccal mucosal wound healing. *Gels* 8, 385.
- Islam, N., Dmour, I., Taha, M.O., 2019. Degradability of chitosan micro/nanoparticles for pulmonary drug delivery. *Heliyon* 5, e01684.
- Islam, M.M., Ramesh, V.H., Bhavani, D., Goudanavar, P.S., Naveen, N.R., Ramesh, B., Fattepur, S., Shiroorkar, N., Habeebuddin, M., Meravanige, G., Telsang, M., Sreeharsha, N., Durga Bhavani, P., Raghavendra Naveen, N., 2022. Optimization of process parameters for fabrication of electrospun nanofibers containing neomycin sulfate and Malva sylvestris extract for a better diabetic wound healing. *Drug Deliv.* 29, 3370–3383. <https://doi.org/10.1080/10717544.2022.2144963>.
- Karimi, K., Katona, G., Csóka, I., Ambrus, R., 2018. Physicochemical stability and aerosolization performance of dry powder inhalation system containing ciprofloxacin hydrochloride. *J. Pharm. Biomed. Anal.* 148. <https://doi.org/10.1016/j.jpba.2017.09.019>.
- Kaur, J., Muttill, P., Verma, R.K., Kumar, K., Yadav, A.B., Sharma, R., Misra, A., 2008. A hand-held apparatus for “nose-only” exposure of mice to inhalable microparticles as a dry powder inhalation targeting lung and airway macrophages. *Eur. J. Pharm. Sci.* 34. <https://doi.org/10.1016/j.ejps.2008.02.008>.
- Kean, T., Thanou, M., 2010. Biodegradation, biodistribution and toxicity of chitosan. *Adv. Drug Deliv. Rev.* 62, 3–11. <https://doi.org/10.1016/j.addr.2009.09.004>.
- Luo, L.H., Zheng, P.J., Nie, H., Chen, Y.C., Tong, D., Chen, J., Cheng, Y., 2016. Pharmacokinetics and tissue distribution of docetaxel liposome mediated by a novel galactosylated cholesterol derivatives synthesized by lipase-catalyzed esterification in non-aqueous phase. *Drug Deliv.* 23, 1282–1290. <https://doi.org/10.3109/10717544.2014.980525>.
- Máca, J., Jor, O., Holub, M., Sklienka, P., Burša, F., Burda, M., Janout, V., Ševčík, P., 2017. Past and present ARDS mortality rates: A systematic review. *Respir. Care*. <https://doi.org/10.4187/respcare.04716>.
- Mallamma, T., Bharathi, D.R., Lakshmi, R.G., Vyjayanthimala, T., Nagasubbarreddy, J., Naveen, R., 2014. Etoposide-loaded nanoparticles made from poly-ε-caprolactone (PCL): formulation, characterization, in vitro drug release for controlled drug delivery system. *Int. J. Biopharm.* 5, 5–12.
- Nair, A.B., Shah, J., Al-Dhubiab, B.E., Jacob, S., Patel, S.S., Venugopala, K.N., Morsy, M. A., Gupta, S., Attimmarad, M., Sreeharsha, N., Shinnu, P., 2021. Clarithromycin solid lipid nanoparticles for topical ocular therapy: optimization evaluation and in vivo studies. *Pharmaceutics* 13. <https://doi.org/10.3390/PHARMACEUTICS13040523>.
- Naveen, N.R., Nagaraja, T.S., Bharathi, D.R., Reddy, J.N.S., 2013. Formulation design and in vitro evaluation for stomach specific drug delivery system of anti retroviral drug-acyclovir. *Int. J. Pharm. Life Sci.* 4, 2506–2510.
- Naveen, N.R., Gopinath, C., Rao, D.S., 2017. Design expert supported mathematical optimization of repaglinide gastroretentive floating tablets: In vitro and in vivo evaluation. *Futur J. Pharm. Sci.* <https://doi.org/10.1016/j.fjps.2017.05.003>.
- Patton, J.S., Fishburn, C.S., Weers, J.G., 2004. The lungs as a portal of entry for systemic drug delivery. *Proc. Am. Thorac. Soc.* <https://doi.org/10.1513/pats.200409-049TA>.
- Popoola, L.T., 2019. Nano-magnetic walnut shell-rice husk for Cd(II) sorption: design and optimization using artificial intelligence and design expert. *Heliyon* 5. <https://doi.org/10.1016/j.heliyon.2019.e02381>.
- Powers, K., 2022. Acute respiratory distress syndrome. *J. Am. Acad. Physician Assist* 35. <https://doi.org/10.1097/01JAA.0000823164.50706.27>.
- Raghavendra Naveen, N., Anitha, P., Gowthami, B., Goudanavar, P., Fattepur, S., 2023. QbD assisted formulation design and optimization of thiol pectin based Polyethyleneglycol and Montmorillonite(PEG/MMT) nanocomposite films of neomycin sulphate for wound healing. *J. Drug Deliv. Sci. Technol.* 82. <https://doi.org/10.1016/j.jddst.2023.104348>.
- Rasul, R.M., Tamilarasi Muniandy, M., Zakaria, Z., Shah, K., Chee, C.F., Dabbagh, A., Rahman, N.A., Wong, T.W., 2020. A review on chitosan and its development as pulmonary particulate anti-infective and anti-cancer drug carriers. *Carbohydr. Polym.* 250. <https://doi.org/10.1016/j.carbpol.2020.116800>.
- Rathore, A.S., Winkle, H., 2009. Quality by design for biopharmaceuticals. *Biotechnol. Nat. Biotechnol. Nat.* <https://doi.org/10.1038/nbt0109-26>.
- Rizg, W.Y., Naveen, N.R., Kurakula, M., Bukhary, H.A., Safhi, A.Y., Alfayez, E., Sindi, A. M., Ali, S., Murshid, S.S., Hosny, K.M., 2022. QbD supported optimization of the alginate-chitosan nanoparticles of simvastatin in enhancing the anti-proliferative activity against tongue carcinoma. *Gels* 8, 103.
- Rowley, J.A., Madlambayan, G., Mooney, D.J., 1999. Alginate hydrogels as synthetic extracellular matrix materials. *Biomaterials* 20. [https://doi.org/10.1016/S0142-9612\(98\)00107-0](https://doi.org/10.1016/S0142-9612(98)00107-0).
- Rubinfeld, G.D., Caldwell, E., Peabody, E., Weaver, J., Martin, D.P., Neff, M., Stern, E.J., Hudson, L.D., 2005. Incidence and outcomes of acute lung injury. *N. Engl. J. Med.* 353. <https://doi.org/10.1056/nejmoa050333>.
- Salatin, S., Jelvehgari, M., 2021. Expert design and optimization of Ethyl Cellulose-Poly (ε-Caprolactone) blend microparticles for gastro-retentive floating delivery of metformin hydrochloride. *Curr. Drug Deliv.* 18, 1137–1147. <https://doi.org/10.2174/1567201818666210204164145>.
- Satyavert, G., Choudhury, H., Jacob, S., Nair, A.B., Dhanawat, M., Munjal, K., 2021. Pharmacokinetics and tissue distribution of hydrazinocurcumin in rats. *Pharmacol. Rep.* 73. <https://doi.org/10.1007/s43440-021-00312-5>.
- Schafroth, N., Arpagaus, C., Jadhav, U.Y., Makne, S., Douroumis, D., 2012. Nano and microparticle engineering of water insoluble drugs using a novel spray-drying process. *Colloids Surf. B Biointerfaces* 90. <https://doi.org/10.1016/j.colsurfb.2011.09.038>.
- Shah, J., Nair, A.B., Jacob, S., Patel, R.K., Shah, H., Shehata, T.M., Morsy, M.A., 2019. Nanoemulsion based vehicle for effective ocular delivery of moxifloxacin using experimental design and pharmacokinetic study in rabbits. *Pharmaceutics* 11. <https://doi.org/10.3390/pharmaceutics11050230>.
- Sharma, R., Saxena, D., Dwivedi, A.K., Misra, A., 2001. Inhalable microparticles containing drug combinations to target alveolar macrophages for treatment of pulmonary tuberculosis. *Pharm. Res.* 18. <https://doi.org/10.1023/A:1012296604685>.
- Sreeharsha, N., Hiremath, J.G., Prashanth Kumar, R., Meravanige, G., Khan, S., Karnati, R.K., Attimmarad, M., Al-Dhubiab, B., Nair, A.B., Venugopala, K.N., 2021. Doxorubicin hydrochloride loaded polyanhydride nanoformulations and cytotoxicity. *Indian J. Pharm. Educat. Res.* 55, 1–9. <https://doi.org/10.5530/ijper.55.1.2>.
- Sreeharsha, N., Naveen, N.R., Anitha, P., Goudanavar, P.S., Ramkanth, S., Fattepur, S., Telsang, M., Habeebuddin, M., Answer, M.K., 2022. Development of nanocrystal compressed minitables for chronotherapeutic drug delivery. *Pharmaceutics* (Basel) 15. <https://doi.org/10.3390/ph15030311>.
- Torge, A., Pavone, G., Jurisic, M., Lima-Engelmann, K., Schneider, M., 2019. A comparison of spherical and cylindrical microparticles composed of nanoparticles for pulmonary application. *Aerosol Sci. Tech.* 53. <https://doi.org/10.1080/02786826.2018.1542484>.
- Villar, J., Blanco, J., Kacmarek, R.M., 2016. Current incidence and outcome of the acute respiratory distress syndrome. *Curr. Opin. Crit. Care*. <https://doi.org/10.1097/MCC.0000000000000266>.
- Waljee, A.K., Rogers, M.A.M., Lin, P., Singal, A.G., Stein, J.D., Marks, R.M., Ayanian, J.Z., Nallamothu, B.K., 2017. Short term use of oral corticosteroids and related harms among adults in the United States: population based cohort study. *BMJ* 357. <https://doi.org/10.1136/bmj.j1415>.
- Wang, X., Wan, W., Lu, J., Zhang, Y., Quan, G., Pan, X., Wu, Z., Liu, P., 2022. Inhalable cryotranshionone spray-dried swellable microparticles for pulmonary fibrosis therapy by regulating TGF-β1/Smad3, STAT3 and SIRT3 pathways. *Eur. J. Pharm. Biopharm.* 172. <https://doi.org/10.1016/j.ejpb.2022.02.012>.
- Wang, H., Xu, Y., Zhou, X., 2014. Docetaxel-loaded chitosan microspheres as a lung targeted drug delivery system: In vitro and in vivo evaluation. *Int. J. Mol. Sci.* 15. <https://doi.org/10.3390/ijms15033519>.
- Yu, L.X., Amidon, G., Khan, M.A., Hoag, S.W., Polli, J., Raju, G.K., Woodcock, J., 2014. Understanding pharmaceutical quality by design. *AAPS J.* <https://doi.org/10.1208/s12248-014-9598-3>.